ADAPTIVE LOCAL TONE MAPPING OF COLOR IMAGES

Radu Ciprian Bilcu, Sakari Alenius and Markku Vehvilainen

Nokia Research Center, Visiokatu 1, 33720, Tampere, Finland.

ABSTRACT

In this paper we propose an adaptive method for local tone mapping in which the vicinity of the current pixel is adaptively selected in order to reduce the artifacts near edges. In addition to that, the only parameter controlling the global effect of the tone mapping is adaptively computed based on the statistics of the processed image. To introduce our method, we start from a simple analysis of the tone mapping model and we validate our method by experimental results. Finally, we compare our method with an existing local tone mapping approach.

Index Terms— Image processing, image tone mapping.

1. INTRODUCTION

Nowadays the mobile devices market is growing fast with many devices being launched on the market. Almost all mobile devices (such as mobile phones and PDAs) are now equipped with digital cameras of various sizes providing better and better image quality. However, due to the size and production cost limitations encountered in the mobile devices, there are several factors influencing the quality of the captured images. One of them is the moderate dynamic range of the imaging sensor which highly influences the quality of the captured images. The images captured with such sensors very often contain regions that are too dark and suffer from a reduced overall contrast.

There are many tone mapping approaches in the open literature that try to solve the low contrast problem. They can be categorized into global and local methods. In the case of global tone mapping solutions usually the histogram of the pixel values are build and a tone mapping function is obtained based on the histogram [1–5]. The global tone mapping algorithms have low computational complexity but provide lower visual quality compared to the local tone mapping solutions. In some local tone mapping implementations the pixel values and the local averages of the image are utilized to modify the pixel intensities [6, 7]. Other solutions to the local tone mapping problem are using non-linear filtering [8], histogram equalization of local windows of the image [9, 10] or combinations of global and local operators [11–13]. The local tone mapping methods usually ensure a better visual quality of the processed image but at the expense of increased computational complexity and processing power.

In this paper we propose a novel adaptive method for local tone mapping of color images. To develop our method, we start from the approach of [7] and we extend this method introducing two adaptive mechanisms to estimate the parameters of the mapping function based on the statistics of the input image.

2. EXISTING APPROACH

In this section we briefly describe the local tone mapping method from [7], to which our method is closely related. Although the method of [7] have been introduced for processing RAW image data, the model utilized has a good performance when applied also for interpolated color images. In order to preserve the original colors, the tone mapping is applied only to the intensity component and the output color image is obtained by nonlinear transformation of the original color components. In this section we describe only the tone mapping procedure applied to the intensity component and the implementation details for color images are given in the next section.

The intensity component of the input image is denoted as $Y(i,j)$ and the output pixel intensity is denoted by $Y_o(i,j)$, with (i,j) being the pixel coordinates. In [7] the following function is utilized to map the values of $Y(i,j)$ to the new values $Y_o(i,j)$:

$$Y_o(i,j) = \frac{max + Y_m(i,j) + R}{Y(i,j) + Y_m(i,j) + R} Y(i,j) \qquad (1)$$

where max is the maximum value of $Y(i,j)$, $Y_m(i,j)$ is the smoothed version of $Y(i,j)$ (here the $N \times N$ smoothing filter has a Gaussian shape with variance $\sigma^2 = N/4$ as suggested in [7]) and R is a regularization term that controls the global effect of the mapping process.

In [6] and [7] the effect of the window size N and the effect of the term R have been analyzed. If the size of the local window is large the local contrast is increased while a too small value of N does not increase the local contrast of the image. However, large window sizes introduce halo artifacts around the edges of the image. In [6, 7] the tone mapping equation (1) is recursively applied two times with different

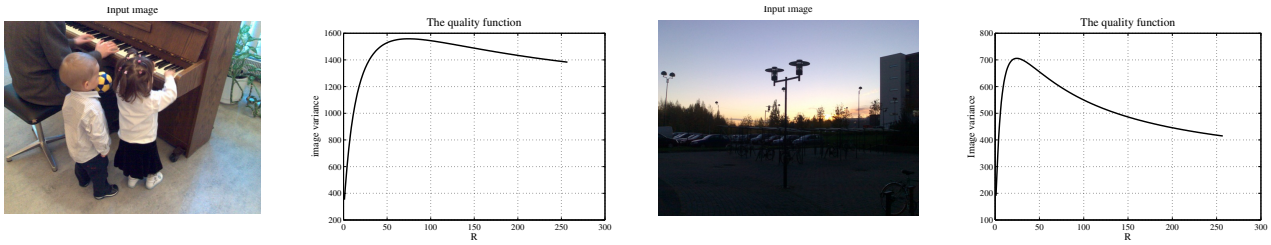

Fig. 1. Example of two images (left) and the corresponding quality functions (right).

values of N. The parameter R is selected as half of the average of $Y(i,j)$ in [7]. The reason for this selection is that small values of R will strengthen the global tone mapping effect and increase more the brightness of the processed image compared to a larger R.

Although this method has a good performance we believe that it suffers from two drawbacks related to the selection of the parameters N and R. These drawbacks are addressed in the next section.

3. PROPOSED METHOD

3.1. Tone mapping regularization

In order to introduce our method lets first analyze (1) where the function used to transform the intensity of the input image is defined. First off all, we are interested to compute the effect of (1) for two different values of the regularization R. Lets denote by $Y_o^{(1)}$ the intensity computed using R_1 and by $Y_o^{(2)}(i,j)$ the intensity computed using R_2:

$$Y_o^{(1)}(i,j) = \frac{max + Y_m(i,j) + R_1}{Y(i,j) + Y_m(i,j) + R_1} Y(i,j),$$
$$Y_o^{(2)}(i,j) = \frac{max + Y_m(i,j) + R_2}{Y(i,j) + Y_m(i,j) + R_2} Y(i,j). \quad (2)$$

In (2) the same local average $Y_m(i,j)$ is used in the computation of both $Y_o^{(1)}(i,j)$ and $Y_o^{(2)}(i,j)$. After some simple mathematical manipulations it can be shown that:

$$Y_o^{(1)}(i,j) \leq Y_o^{(2)}(i,j) \quad \text{if} \quad R_1 \geq R_2. \quad (3)$$

The output intensity for very large values of R can be computed, from (1) as:

$$\lim_{R\to\infty} (Y_o(i,j)) = \lim_{R\to\infty} \left(\frac{max + Y_m(i,j) + R}{Y(i,j) + Y_m(i,j) + R} Y(i,j) \right)$$
$$= \lim_{R\to\infty} (Y(i,j)) = Y(i,j). \quad (4)$$

From (3) one can see that if the value of the parameter R decreases, the value of $Y_o(i,j)$ increases, respectively. There are two effects influencing the contrast and the variance of $Y_o(i,j)$. Pixels having low intensity values will be redistributed towards higher intensities, when R decreases. This has the effect of increasing the contrast and the variance of the dark parts of the image. On the other hand, the pixels with high intensities will accumulate closer to the maximum value max (noting that the range of $Y_o(i,j)$ is limited to the range of $Y(i,j)$) and the effect is the decrease of the contrast and variance of the bright parts of the image.

As a consequence, from these two opposite effects, one can expect that the variance and the contrast of the processed image as a function of parameter R will have a maximum for a certain value of R which depends on the distribution of the pixel values. In our approach, we use the variance of the processed image as a measure of the overall contrast although other methods can be utilized as well. The image variance will then be used to select the optimum R adaptively. Equation (1) is applied with different values of R and the variance of $Y_o(i,j)$ is computed each time. The optimal value of R is selected to be the one which gives the largest variance. Since R is a nonnegative parameter and values larger than the maximum of $Y(i,j)$ does not bring a substantial change in the contrast the search range for R is limited to $[0, max]$.

The behavior of the variance of the processed intensity component has been tested for a large database containing several types of images. For illustration purposes, in Fig. 1 we show two examples of input images together with the plots of the variances as functions of the parameter R. We can see from these examples that the quality function (the image variance) has a maximum for a certain value of R which is different from one image to another. In one image the algorithm selected $R = 148$ which is 1.34 times the intensity average, while in the second image the value of the parameter was selected 0.47 times the average of the intensity component. Both examples and also the other tests we have done are in agreement to the theoretical analysis presented above.

Fig. 2. The input image (left), the image processed by [7] (middle), and the image processed by our method (right).

Fig. 3. The input image (left), the image processed by [7] (middle), and the image processed by our method (right).

3.2. Local adaptivity

The second drawback of the method in [7] is that a too large local window size N causes halo artifacts at edges. Our method for size selection is based on the Intersection of the Confidence Interval (ICI) and is similar to the one previously published in [14].

We select a set of M different window sizes denoted as $[N_1, \ldots, N_M]$ and the following steps are implemented for size adaptation:

1. For a given pixel $Y(i,j)$ compute the corresponding averages $Y_m(i,j,k)$ for each of the pre-defined window sizes N_k, $k = 1, \ldots, M$, where the index k is used to identify the size from the set $[N_1, \ldots, N_M]$.

2. The confidence interval for each computed average is defined as:

$$B_k(i,j) = \left[Y_m(i,j,k) - \Gamma\sigma_n^2, Y_m(i,j,k) + \Gamma\sigma_n^2\right]. \quad (5)$$

where Γ is a constant parameter (typically selected as $\Gamma = 1.2$, [14]) and σ_n^2 is the variance of the additive noise (we have estimated the noise variance using the method from [15]).

3. Starting from $k = 2$ the intersection of every two adjacent intervals $B_{k-1}(i,j)$ and $B_k(i,j)$ is verified. If the two adjacent intervals have at least a point in common the interval $B_k(i,j)$ is updated such that it contains only the common points and the process continues for the next value of k. Otherwise, the optimum window is selected as $N_{opt} = N_{k-1}$.

The above mentioned steps are utilized to select the local window size for each pixel from the image. The local averages $Y_m(i,j,k)$ are computed by weighting the selected pixels with a Gaussian-shaped PSF of the size selected by the above algorithm.

3.3. Proposed algorithm

In order to implement our adaptive tone mapping method, the following procedure is implemented:

1. The input color image with the red, green, and the blue components $I(i,j,1)$, $I(i,j,2)$, and $I(i,j,3)$ is transformed first in the YUV domain and only the $Y(i,j)$ component is processed further.

2. The algorithm from Section 3.2 for selecting the sizes of the local windows is utilized to estimate the optimum size for each pixel $Y(i,j)$.

3. The image of the local averages $Y_m(i,j)$ is computed using the optimum local window sizes.

4. The computed local averages $Y_m(i,j)$ are utilized to estimate the optimum value R_{opt} according to the procedure from Section 3.1.

5. The tone mapped component $Y_o(i,j)$ is computed using $Y_m(i,j)$ and R_{opt}, obtained in steps 3 and 4, as:

$$Y_o(i,j) = \frac{max + Y_m(i,j) + R_{opt}}{Y(i,j) + Y_m(i,j) + R_{opt}} Y(i,j) \quad (6)$$

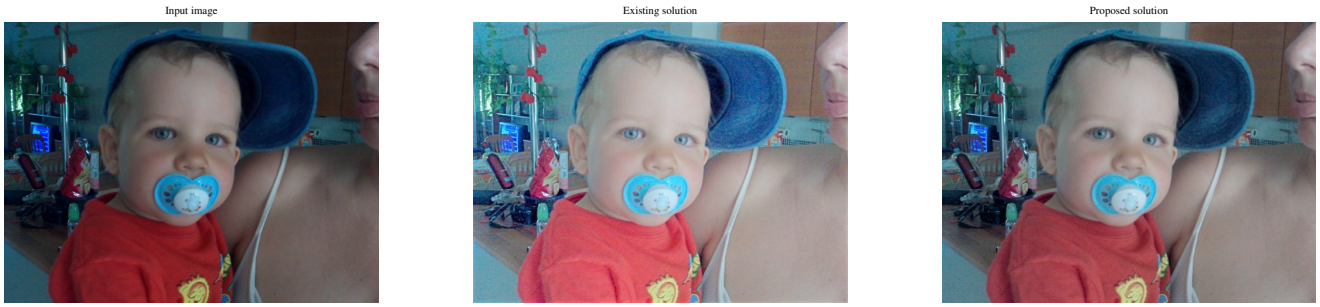

Fig. 4. The input image (left), the image processed by [7] (middle), and the image processed by our method (right).

Fig. 5. The input image (left), the image processed by [7] (middle), and the image processed by our method (right).

6. The output color components $I_o(i,j,1)$, $I_o(i,j,2)$ and $I_o(i,j,3)$ are obtained as:

$$I_o(i,j,t) = I(i,j,t)\left(\frac{Y_o(i,j)}{Y(i,j)}\right)^{\gamma}, \qquad t = 1,2,3 \quad (7)$$

with γ being the gamma correction parameter that ensures appropriate color rendering for different displays.

4. EXPERIMENTS AND RESULTS

We have done extensive simulations on a large image database in order to validate the theoretical considerations from Section 3 and also to compare our method with the solution of [7]. While, in Section 3 we have presented the validation experiments, in this section we mainly focus on comparing the two addressed algorithms.

In Fig. 2 we show the input image and images processed with the approach from [7] and with our solution. We have selected this image in order to show the behavior of both algorithms on underexposed images. We can see from this figure that our method ensures a more natural look of the processed image. This is due to the fact that a value of R equal to the half of the image average leads to a too much increase of the image luminance (a value of $R = 40$, which is 1.29 times the image average has been selected by our method). Note also reduced halo effects at edges due to local adaptivity in our solution.

Fig. 6. Part of an image processed by [7] (left), the corresponding part of the image processed by our method (right).

In Fig. 3 we show an example in which a correctly exposed image has been captured and processed with both compared algorithms. Also in this case our proposed method gives better visual quality compared to the solution from [7] which increases too much the overall brightness of the processed image. Other example images showing the performance of our

method compared with the approach in [7] are shown in Fig. 6 and Fig. 4.

To illustrate the reduced halo effect of our proposed method, in Fig. 6 we show a parts of the images depicted in Fig. 2. One can see that our method has reduced halo artifacts near the high contrast edges.

5. CONCLUSIONS

In this paper we have proposed a novel method for local tone mapping of color images. Our method uses two adaptive control parameters to increase the visual quality of the processed images. One parameter is the spatial range of the local adaptation, that is the optimal size N of the neighborhood affecting the global tone mapping effect. The other parameter, R, controls the strength of the local tone mapping function. This value is optimized based on the image variance. In our method, thanks to the optimally chosen parameters, it is possible to use only one tone mapping step instead of two. Although the original method of [7] uses a two-layer model, we have deliberately chosen a one-layer model, because of the parameter optimization procedure. This results in an increase of the image contrast and a reduction of the halo effect.

We have presented the theoretical analysis of the utilized model and validated the analysis by experiments. We also compared our method with a similar approach and shown that it can provide better visual quality of the processed images.

6. REFERENCES

[1] F. Drago, K. Myszkowski, T. Annen, and N. Chiba, "Adaptive logarithmic mapping for displaying high contrast scenes," in *Proc. of EUROGRAPHICS*, Granada, Spain, 2003, EUROGRAPHICS, pp. 419–426.

[2] J. Duan and G. Qiu, "Fast tone mapping for high dynamic range images," in *Proc. of Int. Conf. on Patt. Rec.*, Cambridge, UK, 2004, IEEE, pp. 847–850.

[3] T.-C. Jen, B. Hsieh, and S.-J. Wang, "Image contrast enhancement based on intensity-pair distribution," in *Proc. of the Int. Conf. on Im. Proc.* IEEE, 2005, pp. 913–916.

[4] Y.-T. Kim, "Contrast enhancement using brightness preserving bi-histogram equalization," *IEEE Trans. on Cons. El.*, vol. 43, pp. 1–8, February 1997.

[5] T. Kim and H. S. Yang, "Colour histogram equalization via least-squares fitting of isotropic gaussian mixture to uniform distribution," *IEEE El. Lett.*, vol. 42, pp. 452–454, April 2006.

[6] D. Tamburrino, D. Alleysson, L. Meylan, and S. Susstrunk, "Digital camera workflow for high dynamic range images using a model of retinal processing," in *Proc. Elec. Im.: Dig. Photo. IV*, San Jose, CA, USA, 2008, IS&T/SPIE.

[7] L. Meylan, D. Alleysson, and S. Susstrunk, "Model of retinal local adaptation for the tone mapping of color filter array images," *J. of Opt. Soc. of America*, vol. 24, pp. 2807–2816, September 2007.

[8] T. Arici and Y. Altunbasak, "Image local contrast enhancement using adaptive non-linear filters," in *Proc. of Int. Conf. on Image Proc.* IEEE, 2006, pp. 2881–2884.

[9] L.-S. Kim J.-Y. Kim and S.-H. Hwang, "An advanced contrast enhancement using partially overlapped sub-block histogram equalization," *IEEE Trans. on Circ. and Syst. for Video Tech.*, vol. 11, pp. 457–484, April 2001.

[10] J. Duan, M. Bressan, C. Dance, and G. Qiu, "Tone-mapping high dynamic range images by novel histogram adjustment," *Pattern Recognition*, vol. 43, pp. 1847–1862, 2010.

[11] M. Ashikhmin, "A tone mapping algorithm for high contrast images," in *Proc. of the 13th Eurographics workshop on Rendering*. Eurographics, 2002, pp. 1–11.

[12] C. Liu, O. Au, C. Cheng, and K. Yip, "Two-level optimized tone mapping for high dynamic range images," in *Proc. of the Int. Conf. on Im. Proc.*, Hong Kong, 2010, IEEE, pp. 3153–3156.

[13] E. Reinhard, M. Stark, P. Shirley, and J. Ferwerda, "Photographic tone reproduction for digital images," *ACM Trans. on Graph.*, vol. 21, 2002.

[14] R. C. Bilcu, S. Alenius, and M. Vehvilainen, "Combinned De-noising and Sharpening of Color Images in DCT domain," in *Proc. of IEEE Int. Conf. on Dig. Sig. Proc.*, Santorini, Greece, july 2009, IEEE.

[15] R. C. Bilcu and M. Vehvilainen, "A New Method for Noise Estimation in Images," in *Proc. of Int. Work. on Nonlinear Sig. and Im. Proc.*, Saporo, Japan, May 2005, IEEE-EURASIP.

[16] F. Durand and J. Dorsey, "Interactive tone mapping," in *Proc. of the Eurographics Work. on Render. Tech.*, 2000.

[17] P. Ledda, A. Chalmers, and et al., "Evaluation of tone mapping operators using a high dynamic range display," *ACM Transactions on Graphics*, vol. 24, pp. 640–648, 2005.